

26 

UCRL-50158

UNIVERSITY OF CALIFORNIA  
Lawrence Radiation Laboratory  
Livermore, California

AEC Contract No. W-7405-eng-48

NUMERICAL STATISTICAL MECHANICS\*

Berni J. Alder and William G. Hoover

January, 1967

\*Work performed under the auspices of the U.S. Atomic Energy Commission.

## I. INTRODUCTION

It has been evident ever since the formulation of statistical mechanics that progress toward a quantitative theory of liquids is limited by mathematical and not conceptual difficulties. The advent of large-scale computers has vastly increased the power of numerical, if not mathematical, techniques and it is therefore natural to ask what additional contribution to the understanding of liquids can be made through the computer. In this review we wish to discuss the impact the numerical methods have had in a general way, referring to the literature or future publications for most details. The numerical method principally referred to is the molecular dynamic calculation although comparisons will be made to Monte Carlo calculations.

This impact can be discussed only if the essential limitations of the computer schemes are kept in mind. One of these is that the potential of interaction between the particles making up the system is pair-wise additive. Although this is not a necessary restriction, all the investigations so far have employed it because of the great simplification that ensues. Another enormous complication that has not been effectively overcome is the description of systems that behave quantum mechanically. Although schemes to deal with this situation can be formulated, they are all cumbersome, particularly in taking the wave-function symmetry requirements of quantum statistics into account. Another limitation concerns the relatively small number of degrees of freedom that can be dealt with on even the largest conceivable computer. This limitation does not turn out to be serious in most situations and can in fact be turned to advantage by studying how various properties depend on the number of degrees of freedom. Finally, the relatively short physical time for which molecular dynamics calculations can be pursued limits applications to processes having short relaxation times, thus, for example, excluding studies in hydrodynamics.

With these limitations, the computer can be used in essentially two ways after restricting the subsequent discussion to classical systems. Although these two ways are not really distinct, it is necessary to distinguish between them because of the present lack of quantitative knowledge about the potential of interaction. One can either determine the nature of the actual intermolecular potential by comparing computer results with experiments or, alternatively, introduce simple idealized potentials to test and improve theories. Since in most situations the computer calculations for a given potential are at least as accurate as the available data, any quantitative comparison to experiment is necessarily limited by the accuracy with which the potential is known. Hence under these circumstances the best way to use the computer is to find the effective pair potential that fits the data.<sup>1</sup> This is a familiar process in statistical mechanics, previously used whenever analytical expressions were available as, for example, in the solid phase at low temperature<sup>2</sup> and in the dilute gas phase.<sup>3</sup> The computer permits extension of this process over the entire phase diagram and to either transport or equilibrium data. The effective pair potential so obtained can then be compared with pair-wise additive potentials obtained either theoretically or by direct scattering experiments.<sup>1</sup> For insulators, such as argon, the difference between the effective potential and pair-wise additive potential appears to be small; an accurate analysis is required to discover the deviations. For ionic systems, such as salts, and especially metals, the effective potential differs much more from the pair potential. In any case, through the use of the computer it is possible to reduce the quantitative description of actual systems to a quantum-mechanical calculation of the effective pair potential as a function of temperature and density. Although this effective pair potential is difficult to calculate, it represents a useful intermediate

function with which to correlate various properties under given conditions.

The alternate use of the computer, to be explored here, is to abandon temporarily comparison with experiment and instead to study systems which are simple enough to aid theoretical developments. The simplification can only involve the choice of a particular form of a strictly pair-wise additive potential, which nevertheless contains the essential features of a real potential. The computer then generates the properties of this system (comparable to experimental data) together with much more detail about the microscopic behavior than any conceivable experiment could obtain. This extra detail is most valuable in checking models and developing more accurate approximations. As far as the theory of liquids is concerned these computer experiments can accurately establish the properties of a simple model which serves as an "ideal" liquid comparable to the perfect gas and harmonic solid abstractions. It is the lack of such a model amenable to analytical treatment that has made the description of liquids so difficult. The computer generation of detailed properties of this "ideal" liquid can then be looked upon as tabulation of functions with which further analytic developments can be made. These functions can be used as bases for expansions,<sup>4</sup> just as the perfect gas limit serves as a basis for the virial coefficient expansion.

What should this "ideal" liquid be? It is clear from past work that neither the perfect gas nor the harmonic solid is an accurate enough representation of the fluid state to serve even as a good zero-order approximation. This is evident from the later discussion which shows that the cell theories,<sup>5</sup> frequently used for the liquid state in the hope that a solid-like description is adequate, are exact only in the limit where a particle is completely confined to its lattice site.<sup>6</sup> This means that cell theories are accurate only at 0°K or, at any finite temperature, at high enough density so that the kinetic energy is a small fraction of the total free energy. In other words,

cell theories give correct limiting expressions under conditions far from the liquid state. Although, as will be seen, series expansions of thermodynamic properties starting from the exact limiting behavior of cell theories can be made, these series do not converge into the liquid state. An additional difficulty associated with this expansion is that the coefficients have not yet been theoretically formulated.

For the gas phase, the expansion away from its ideal state has long been known as the virial series.<sup>7</sup> In spite of much effort only a few coefficients have been calculated. Many more terms would be required to describe the liquid state adequately, because the perfect gas state is so far removed from the liquid state. An additional problem is that convergence of this expansion into the liquid state is not assured even if all the terms could be calculated. Convergence of the series has been established only for a very dilute gas.<sup>8</sup> Although efforts to evaluate the general term in the expansion have not yet led to concrete results, the computer can and has been used to evaluate a few higher virial coefficients;<sup>9</sup> these calculations will be discussed in detail in a later section. Their relevance to a theory of liquids lies mostly in the establishment of an exact expansion with which approximate calculations can be compared. However, even this comparison can lead to pitfalls since an approximation which does not do well at low density can be quite adequate at high density<sup>10</sup> and vice versa. As far as using the virial coefficients to obtain information on the intermolecular potential is concerned, the calculation of the higher virial coefficients has far outstripped the experimental ability to obtain them accurately.

Since neither the solid nor the gas is an adequate basis for the ideal liquid one might be tempted to describe the liquid as a judicious admixture of the harmonic solid and the perfect gas.<sup>11</sup> This is not very satisfactory either since no admixture represents realistically the most probable state of a fluid. Such schemes should be looked upon as interpolation formulae between

the gas and solid state with empirically determined values of the amount of admixture so as to reproduce some liquid properties. These interpolation schemes can then be useful in predicting other liquid properties.

The hope left now is that the one remaining extreme state, at high temperature and high density, can serve as an ideal liquid. There is indeed experimental evidence to support this hope. The primary piece of evidence is that at constant density the structure of a fluid, as measured by the pair distribution function with x-rays, is nearly independent of temperature.<sup>12</sup> Thus, the high-temperature behavior of a fluid can be used as the "ideal" state, which brings with it the great simplification that only the repulsive part of the potential need be considered in determining the structure and many other properties of the fluid. The attractive part of the potential, if it contributes at all to a given property, need be considered only in the rough sense that it contributes some mean field. Further support for this mean field contention can be obtained by observing that the pair distribution function is nearly independent of the type of attractive forces. For example, even the structure of metallic and ionic systems is nearly the same as that of insulating materials at corresponding densities. For these systems with greatly different attractive forces but similar repulsive forces not only is the structure nearly the same but so is, for example, the viscosity or mass diffusion coefficient.<sup>13</sup> Thus the crucial idealization of all liquids is that their primary behavior is determined by the steep repulsive potential, which can best be itself idealized by an infinitely steep one, namely a hard sphere potential.

The above description of a fluid is one of the oldest in existence, and is commonly associated with the name van der Waals.<sup>14</sup> The van der Waals picture of a fluid corrects the perfect gas theory by taking into account two factors. One of these is that the volume occupied by the particles themselves

at liquid densities can no longer be neglected compared to the volume of the system, so that the accessible volume is the total volume diminished by a covolume,  $Nb$ . The other factor is that the attractive energy can be simply treated as a constant cohesive energy, so that the pressure is diminished by the internal pressure corresponding to this attractive energy density.

The applicability of van der Waals' model of fluids to transport theory has not been so widely recognized. Here again the computer had and will have a central role in establishing the transport properties of the "ideal" hard sphere fluid. The total attractive potential, to the extent that it is uniform, will not affect relaxation processes at all. The van der Waals picture corresponds simply to the kinetic theory picture of transport, where, however, at higher density the collisional flux due to intermolecular forces can no longer be neglected relative to the kinetic flux due to molecular streaming. The Enskog theory<sup>15</sup> of hard spheres treats both kinds of fluxes but, inasmuch as it involves basically an extension of the Boltzmann equation to high density, the molecular chaos approximation is invoked. The numerical consequence of this approximation can at present be assessed only by computer studies.

The overall impact of the computer studies is then to revive two very old models, van der Waals' and Enskog's, for calculating the equilibrium and transport properties of fluids. In the subsequent sections it is shown in more detail how various computer experiments have helped to confirm the basic physical notions behind these early hypotheses and how these models need to be improved. It is interesting to comment that many of the fluid theories proposed in recent years were motivated primarily by the fact that the model could be represented by a relatively simple mathematical form and that once this restriction to simple mathematics is removed through the use of the computer, it becomes feasible to find out what physical processes are important contributors to various properties.

## II. THE VAN DER WAALS' MODEL

The van der Waals' equation can be written in the following form

$$\frac{pV}{NkT} = \frac{v}{v-b} - \frac{a}{vkT}$$

from which it can be seen that  $\frac{pV}{NkT}$  is made up of two terms. The first one,  $\frac{v}{v-b}$ , is the purely geometric covolume factor, which accounts for the packing of particles in a container. It is this term which the van der Waals' theory approximates very crudely and which can now be replaced, through the data from computer studies, by the value of  $\frac{pV}{NkT}$  for hard spheres.<sup>16</sup> The second factor accounts for the change in pressure due to the fact that the cores can be considered as being immersed in a constant attractive potential,  $-\frac{a}{v}$ .

The above form of the van der Waals' equation and the physical basis on which it is derived both suggest what a theoretical derivation shows explicitly, namely that an expansion in powers of the reciprocal temperature is being represented with the square and higher terms left out. The theoretical derivation<sup>4</sup> of the van der Waals' equation is based on treating the attractive potential as a perturbation on the hard core potential. In this derivation the expansion parameter is the strength of the attractive potential relative to  $kT$ . First order perturbation theory leads to a theoretical expression for  $\underline{a}$ . Insofar as the expansion parameter is small, the higher terms can be neglected and the van der Waals' equation is correct in assuming that the attractive energy does not modify the structure of the fluid as determined by the hard sphere interactions alone. Because the pair distribution function is found to be nearly temperature independent, it can be anticipated that the higher-order expansion terms are quite small. An alternative way to derive the van der Waals' equation rigorously is to make the assumption that the attractive forces are weak and long range.<sup>17</sup> The weak condition insures that

the higher terms in the expansion do not appear. The long-range condition is necessary to make  $a$  constant. If the attractive potential is of long enough range, the potential energy will not vary from one configuration of the particles to another, making rigorous the concept of a mean field leading to a constant energy density.

In order to verify the van der Waals' equation experimentally, the conditions under which it is expected to be accurate must be established. Inasmuch as the maximum depth of the potential corresponds to a temperature slightly smaller than the critical temperature, the weak condition is satisfied down to a temperature somewhat in excess of the critical one. Furthermore, the potential can be considered long range whenever the density is high enough so that the particles are on the average separated by a distance less than the range of the forces (so that the attractive potentials of neighboring particles all overlap). Under these circumstances the attractive potential energy does not differ for most of the more probable configurations. Since the range of the forces is typically 1.5 times the diameter for the rare gases, the attractive forces will all overlap when the volume is less than  $(1.5)^3$  times the 0°K crystalline volume. This crystalline volume does not differ much from the liquid volume at the melting point. Since the critical volume is roughly 3 times the melting volume for the rare gases, the van der Waals' theory should be accurate at densities and temperatures greater than the critical density and temperature.

It is now possible to verify the applicability of the van der Waals' model by checking upon three of its predictions. First of all, a plot of  $\frac{pV}{NkT}$  vs.  $\frac{1}{T}$  should give at high enough densities a straight line down to temperatures near the critical temperature and the infinite temperature intercept should be the hard sphere equation of state. This can be demonstrated best by computer studies because a repulsive potential can be introduced that

has a hard core. In actual systems the repulsive potential is somewhat soft,<sup>1</sup> so that the effective core size shrinks as the temperature increases, causing deviations from straight line behavior. Furthermore, extrapolation to infinite temperature is not to be taken literally for actual systems, because the system disintegrates at high temperatures into electrons and nuclei. Nevertheless, in order for the van der Waals' model to be useful, the concept of an effective core size must be definable over a considerable temperature and density interval. Fig. 1 demonstrates that the straight-line prediction of van der Waals is verified for a square-well potential on the computer down to temperatures near the critical temperature and that deviations even down to liquid temperatures are not very large. This system had a square-well potential with a range of 1.5 times the hard core diameter, a critical temperature,  $T^*$ , of about 1.3 well depths, and a critical volume relative to the close-packed volume,  $v/v_0$ , of about 4.5. For actual systems the equivalent graph, Fig. 2, shows a slight curvature at high temperatures, which can be traced to the above mentioned effect of a decreasing core size with increasing temperature; the latter effect was estimated from the approximately known pair interaction potential in relationship to the kinetic energy. Although the effective core size was found to be dependent on temperature, it was independent of density, as it must be in order for the concept to have meaning. In practice, the effective core size is determined by a comparison of the high temperature intercept of  $\frac{pV}{NKT}$  at a given density with the known hard sphere equation of state. The computer thus made an essential contribution by calculating accurate hard sphere equilibrium properties which could replace van der Waals' crude approximation.

The next prediction of van der Waals that  $a$  is constant, not only independent of temperature but density as well, could also be investigated through

computer calculations. Perturbation theory gives an expression for  $\underline{a}$  involving an integral of the product of the hard sphere radial distribution function and the perturbation potential.<sup>4</sup> The hard sphere radial distribution function has been tabulated from computer runs at various densities, and the attractive part of the square-well potential was taken as the perturbation potential. The straight line drawn in Fig. 1 corresponds to the value of  $\underline{a}$  calculated in this way. The agreement with the points at high temperatures (obtained directly through the virial theorem) merely illustrates consistency between the two different types of computer calculations. Table I then shows how this value of  $\underline{a}$  varies with density. The column labeled  $a_1$  is the above mentioned integral representing the excess internal energy due to the attractive perturbation potential. If  $a_1$  were independent of density the van der Waals  $\underline{a}$  occurring in the equation of state,  $a_2$ , would be identical to  $a_1$  and therefore also a constant. Table I then shows that to a good approximation  $a_1$  is a constant over the entire density range of the system from infinite dilution to the close-packed solid. The approximation is even more accurate in the restricted range of densities appropriate to the van der Waals' model, namely densities greater than critical ( $v/v_0 < 4.5$ ). For potentials of longer range,  $a_1$  was found to be, as expected, more nearly constant over a larger density interval as Table I shows.

At low densities  $a_1$  has been evaluated by substituting the known virial expansion of the hard sphere radial distribution function in the integrand. At high densities  $a_1$  approaches the value of half the number of particles which lie within the range of the forces of a given particle. At intermediate densities the integral was evaluated numerically. Inasmuch as  $a_1$  is nearly constant the agreement with the value of  $a_2$  and its near constancy is to be expected. Strictly speaking, however,  $a_1$  is only constant within the range of the second virial coefficient and hence  $a_1$  and  $a_2$  agree only exactly in

the low density limit. Nevertheless, the van der Waals' assumption of a constant energy density is well justified.

The third prediction of van der Waals, that the coefficient of the next term in the expansion in powers of the reciprocal temperature is small compared to  $\underline{a}$ , could also be verified. The graph in Fig. 1 shows that the deviations from the van der Waals equation are small even at low temperatures indicating that the sum of the contributions of all the terms beyond the ones included in the van der Waals theory is small compared to  $\underline{a}$ . That this should be so can also be made reasonable on physical grounds. The terms omitted by van der Waals depend on the lack of uniformity of the attractive potential sea, that is on the fluctuations in the attractive potential energy. These fluctuations are in turn related to the compressibility of the system. Inasmuch as a liquid is quite incompressible, the omitted terms should be small.

The exact expression from perturbation theory for the coefficient of the square term in the expansion in reciprocal temperatures involves the quadruplet distribution function and therefore, for evaluating its order of magnitude, the superposition approximation has been utilized. This leads to the following equations of state at various densities<sup>18</sup>

$$v/v_0 = 5.136 \quad \frac{pV}{NkT} = 1.83 - \frac{1.88}{T^*} - \frac{0.04}{T^{*2}}$$

$$v/v_0 = 3.196 \quad \frac{pV}{NkT} = 2.67 - \frac{3.29}{T^*} - \frac{0.06}{T^{*2}}$$

$$v/v_0 = 2.097 \quad \frac{pV}{NkT} = 4.33 - \frac{5.35}{T^*} - \frac{0.35}{T^{*2}}$$

$$v/v_0 = 1.728 \quad \frac{pV}{NkT} = 5.56 - \frac{6.54}{T^*} - \frac{0.42}{T^{*2}}$$

These expressions utilize the superposition approximation for all the terms, which is sufficiently accurate for present purposes. The perturbation potential is the attractive part of the Lennard-Jones 12-6 potential; the hard

core diameter corresponds to the distance at which the potential changes sign. The van der Waals' a term, corresponding to the middle term on the righthand side, can be rewritten in the same units as before (the coefficient of  $[T^* \frac{v}{v_0}]^{-1}$ ) as 9.7, 10.5, 11.2, 11.3, respectively, in order of decreasing volume. This not only demonstrates the constancy of van der Waals' a but also its near independence of the nature of the attractive potential (by comparison to the numbers given for the square-well potential in Table I) as long as the range of the forces is comparable. The major point of the above equations is, however, to show that the coefficients of the last term are an order of magnitude less than those of the van der Waals' a term.

Now that the successes of the van der Waals theory have been enumerated, what are its failures? Its greatest failure is that it is unable to predict accurate normal liquid properties. The reason for that is the near cancellation of the hard sphere term by the internal pressure term at low pressures and temperatures, as the above given equations of state clearly show. At temperatures of the order of the well depth ( $T^* \sim 1$ ) the first two terms nearly cancel, so that the pressure is determined by the higher order terms in spite of the fact that these were shown previously to be small. In other words, whenever the pressure is small, an exceedingly accurate solution to the many-body problem is required before quantitative results can be obtained; a feat not yet achieved by any theory. However, this near cancellation of the two terms in the van der Waals' equation does not occur for other thermodynamic properties, such as the internal energy, nor, as shall be seen, for the transport properties. For these the van der Waals' theory is accurate even under normal conditions. This, for example, accounts for the success of Hilderbrand's theory of solubility which is based on energy density calculations.<sup>19</sup> For the equation of state, the van der Waals' theory should be used only at high temperature. In its prediction of high temperature properties it is as successful

a theory as any, provided account is taken of the changing diameter due to the softness of the repulsive intermolecular potential.

The van der Waals' theory also appears to fail in the very small region of long-range correlations and large-scale fluctuations surrounding the critical point. This failure is not surprising in view of the previous remarks that the corrections to the van der Waals' theory depend on the extent of the fluctuations. The computer calculations cannot shed any light on this point, since, in the finite systems studied, the fluctuations are seriously distorted. In fact, a preliminary analysis of the critical point for square-well molecules indicates that the computer systems most probably obey van der Waals' equation very accurately. Not only do the computer calculations predict within the present accuracy a parabolic coexistence curve but they also give a van der Waals' loop in the coexistence region for the microcanonical ensemble used. This effect, due to the surface tension, is to be expected for such systems unless the number of particles and the volume are allowed to go to infinity. Inasmuch as the Maxwell equal area rule can be rigorously justified for a van der Waals' system,<sup>17</sup> the establishment of the coexistence region from the computer runs presents no problem. Finally, it must be pointed out that although the theory fails in the tiny region surrounding the critical point, the van der Waals' equation gives a more accurate value of  $\frac{pV}{NKT}$  at the critical point than many more sophisticated theories.<sup>5</sup>

Previous to the computer studies, the van der Waals theory's greatest failure was thought to be the absence of the melting transition. That phase transition could only be contained within the hard sphere part of the van der Waals' equation, if that theory was to predict melting. The computer studies have made it exceedingly plausible that hard spheres do indeed have such a phase transition.<sup>20</sup> This is the single most important contribution computers

have made to the understanding of equilibrium properties. Together with the other factors mentioned before, the computer transition has reconfirmed the van der Waals' picture of a fluid. Before discussing melting in detail, the van der Waals' picture as applied to fluid transport coefficients will be discussed in the next section. After that, the discussion of melting will naturally lead to a discussion of the behavior of high density systems in the solid phase. Finally, a special section devoted to the region where the van der Waals' equation is inapplicable, namely the low density region, will discuss the virial series and the calculation of virial coefficients by an efficient Monte Carlo procedure.

### III. TRANSPORT PROPERTIES

Existing transport theories can be classified as either low density theories, which attempt to make the equivalent expansion in powers of the density for the transport coefficients (from the low density Boltzmann limit) as was done for the thermodynamic properties by the virial series, or high density theories, which involve some postulated predominant relaxation mechanism. The low density theories have gotten entangled in the mathematical difficulty that the transport properties cannot be expanded in powers of the density;<sup>21</sup> a more complicated expansion is required. Although this observation is extremely interesting in its own right, the physical mechanism leading to this behavior does not appear to be an important contributor to relaxation processes at any density. The physical mechanism involves cyclical collisions in which particles are correlated through having had common collision partners in a chain of events. The molecular dynamics calculation could be used to check upon the probability of such events as a function of density by analyzing the sequence of collisions for closed loops.

The prevalent high density or fluid transport theories assume mechanisms that contradict the van der Waals picture. Whereas the van der Waals' model predicts that the trajectory of a typical particle involves a series of hard

core collisions unaffected by the presence of the attractive forces, recent models for the calculation of the friction constant occurring in Kirkwood's transport theory of liquids have postulated Brownian motion trajectories between hard core collisions.<sup>22</sup> The Brownian motion is said to be caused by many small momentum changes induced by soft collisions, that is by "collisions" with the attractive part of the potential. Thus, instead of the typically linear or free flight trajectory between hard core collisions of the van der Waals' model, a tortuous path involving many small changes in curvature between the large momentum changes of the hard core collisions is thought to be more representative. From a theoretical point of view the difference between these two models is the difference between completely uncorrelated successive hard core collisions and the van der Waals' correlated collisions. Although, naturally, reality lies between those two extremes, molecular dynamics computation on the frequency of different types of collisions strongly favors the van der Waals' picture.<sup>23</sup>

Another view of a typical trajectory of a particle requires an activation energy for flow.<sup>24</sup> The motion of a particle in this model could be abstracted as consisting of a large number of oscillations about some equilibrium position in a cell made up of its immediate neighbors with a rare but large jump (comparable to its own diameter) to a new equilibrium position. The free path distribution obtained from molecular dynamics<sup>25</sup> shows that this popular transport mechanism does not contribute significantly to molecular flow in fluids. Even in a situation favorable for this mechanism, namely in the solid phase, a study of interchanges between holes and particles by molecular dynamics has shown that large jumps do not have any significant probability. The interchanges were, to be sure, found to be rare, but this rarity need not be ascribed to an activation energy in the usual sense of the word. The improbability of

such an interchange can be explained on the basis of the van der Waals' model on purely entropic grounds as due to the infrequency of highly correlated motions among the neighboring particles to a hole in which, by a succession of relatively small moves, a particle can slip by its neighbors into the hole.

On the positive side, the van der Waals model of transport was tested empirically with the additional approximation of molecular chaos; that is, for the transport theory, Enskog's hard sphere theory was used.<sup>26</sup> For a comparison with experiment, it was then only necessary to choose a hard sphere diameter, using equilibrium data as described in the previous section. The numerical agreement within better than 10% for a completely a priori theory was remarkable. Furthermore, the deviations from experiment could be qualitatively understood in that at high temperatures corrections to the Enskog theory of hard spheres predominate while at low temperatures these corrections are nearly cancelled by the ones due to the van der Waals approximation of a constant energy density. The important point, however, is that the corrections are small, and hence that the major contributor to flow is simply motion in small steps (of the order of the mean free path) by a succession of uncorrelated collisions between pairs of particles. Any correlated motion or special mechanism is superimposed on this major contribution, and makes a relatively small numerical contribution to the total flux. This state of affairs implies that it is easy to estimate the order of magnitude of the transport coefficients, and that by numerical agreement with experiment it is hard to prove or disprove any particular mechanism of flow. Thus, rather accurate experiments, such as precise neutron diffraction experiments, are required to detect which of the many special mechanisms that could contribute in fact do. It is here that the method of molecular

dynamics, with its better time and space resolution than any conceivable experiment, can be of enormous help.

The only serious limitation of the computer studies is that spacial correlations extending over much more than 10 molecular diameters would be hard to take into account, because only finite numbers of particles can be handled. Similarly, temporal correlations extending over periods greater than 1000 mean collision times would be hard to detect, because such calculations would take too long. Inasmuch as the relaxation time for the processes leading to the various transport coefficients are between one and two collision times, these limitations do not appear to be serious. Some preliminary studies<sup>27</sup> have been made of the velocity autocorrelation function of hard spheres in order to discover the nature of significant correlated motion at various densities. Much more work is being carried out for this as well as for other autocorrelation functions and for different intermolecular potentials.

The predominant deviation from a Markovian process that appears at high density is an anticorrelating motion previously termed "backscattering"<sup>27</sup>. It signifies the higher than random probability that a particle will have its direction of travel reversed at high density by being scattered back by its surrounding neighbors. The physical effect of this is to slow down the forward flow of particles, thus leading to a decreased diffusion coefficient or increased friction constant. As mentioned before, the comparison of experiment with the Markovian theory at high temperature and density led indeed to predicted transport coefficients which were too high. Another and quantitatively less important structure in the velocity autocorrelation function which was recently observed at intermediate densities is a positively correlated motion occurring quite late, that is, after a time corresponding to about 10 mean relaxation times. It occurs when a hot particle collides

with its neighbors, creating a hot and low density region which persists so long that the formerly hot particle upon being reflected back into that region still finds its density low, and hence preferentially travels on in that direction. This example is a vivid demonstration of the details which a molecular dynamics calculation is capable of exploring.

The accuracy of the van der Waals' model could also be investigated by comparing the velocity autocorrelation function for particles with an attractive potential with the hard sphere one at the same density. The van der Waals' prediction is that they will be nearly the same. This calculation has not yet been carried out. Instead, a more direct test was made in terms of the number of soft versus hard core collisions.<sup>23</sup> At liquid density it was found that the majority of the collisions (about 60%) were hard core collisions nearly independently of the temperature. What did vary with temperature at constant density was that as the temperature was lowered more and more pairs of particles were trapped; that is, their kinetic energy did not suffice to overcome the potential energy binding them. Furthermore, also in accord with van der Waals, the free path distribution was shown to be nearly indifferent to the presence of an attractive potential (see Fig. 3). From the free path distribution, also, it was not possible to pick out any particularly preferred characteristic distance of motion at fluid densities relative to that at gas densities indicating the absence of a vastly different mechanism of flow at any density.

#### IV. MELTING

The van der Waals' model of necessity must associate melting with the hard sphere part of the equation of state. This geometric aspect of melting is another old idea incorporated into the empirical Lindemann law,<sup>28</sup> which successfully accounts for the melting behavior of a very diverse group of substances. Lindemann's law was originally put into the form that a substance melts once the maximum displacement of an atom from its regular lattice site can reach about 10% of the radius of the atom. A cruder way of saying the same thing is that most substances melt upon expanding 30% in volume from their close-packed or 0°K volume. The strange behavior of hard spheres<sup>16</sup> and hard disks<sup>20</sup> found in the neighborhood of these volumes lends confidence both to ascribing the computer observed phenomena as melting and secondly, to the geometric interpretation of melting since it occurred in the absence of attractive forces. Other authors<sup>29</sup> have also recently pointed out the close correspondence between melting of actual substances and the hard sphere transition.

Lindemann's law is usually written in terms of the potential energy at the maximum displacement of an atom in an harmonic oscillator relative to the kinetic energy, where the harmonic force constant is in turn related to the Debye temperature. This expression can be misleading since it obscures the geometric aspect of melting and gives the impression that melting can occur in a purely harmonic force law system. Still another and theoretically suggestive way to express Lindemann's law is in terms of the probability of a density fluctuation of a given size. The main problem, however, in all these equivalent ways of looking at melting is to obtain a theoretical justification for the single empirical constant contained in these proposals, namely, for example, the size of the density fluctuations required before

melting occurs. A physically sensible but difficult way to obtain this constant is through considerations of instability modes in the solid phase as a function of temperature and density. As is well known from the differences in properties of liquids and solids, the solid at melting must become unstable to a long wave length shear mode.<sup>30</sup>

The analysis in such a calculation involves determining instabilities in non-linear equations, the non-linearity being brought on by the anharmonic terms in the force law. Although it is difficult to solve this problem analytically, it is possible by molecular dynamic to confirm at least the validity of the suggested mechanism. For this purpose, first of all, a very simple model which incorporates this point of view was proposed. This model, called the correlated cell model,<sup>31</sup> as opposed to the usual cell model<sup>32</sup> where all the neighboring particles are uncorrelated with the central particle by being kept fixed at their lattice position, treats the central particle as completely correlated with some of its neighbors while the others are kept fixed at their lattice position. In a two-dimensional system of hard disks, the particles were arranged to be so correlated that rows of atoms move relative to each other, each row moving as a unit. The consequences of this model could be worked out very simply analytically and led to a remarkably accurate description of the thermodynamic properties of the solid phase, including melting. A van der Waals-like loop was observed very near the pressure and density where the molecular dynamics result gave a van der Waals-like loop. This loop occurred at a density in the model where one row of atoms could just slip by the neighboring two rows of atoms which at higher density had all been interlocked. This model thus graphically combines the geometric aspect of melting with a shear instability (slipping).

Striking confirmation of the occurrence of this slipping mode at the onset of melting comes from molecular dynamics studies of the singlet distribution function in the hard disk solid phase. The singlet distribution function is the probability of an excursion of a particle from its lattice site in a given direction by a given distance in a solid whose center of mass is fixed. As Fig. 4 shows, a particle has a small probability of being found at a neighboring lattice site at a solid density very close to melting. This jump to neighboring lattice sites corresponds to a row of atoms cooperatively sliding one notch relative to another row. At all densities slightly higher than the melting density this process becomes so improbable that no evidence of this phenomena can be observed in the singlet distribution function which is, in fact, for all practical purposes found to be a spherically symmetric Gaussian.

This spherical symmetry indicates first of all that no one-particle cell theory can adequately calculate the singlet distribution function. The prediction of any such cell theory for hard disks would lead to a flat topped singlet distribution function with sharp sides having the symmetry of the lattice. The fact that this does not correspond to the facts means that the singlet distribution function is primarily determined by the low-frequency density fluctuations which are not sensitive to the local structure. It is for this reason that this singlet distribution function is a delicate indicator of melting. However, for the purposes of calculating thermodynamic behavior of a solid, it is not necessary to be precise about the low-frequency modes, since the thermodynamic properties are primarily determined by the high-frequency modes. It is for this reason that melting comes as such a sudden surprise when evidence is sought on thermodynamic grounds just previous to melting. It is also for this reason that a cell theory can yield accurate

thermodynamic properties without leading either to a qualitatively correct singlet distribution function or to melting. The correlated cell model by adequately representing the high frequency behavior of a solid as well as allowing a low frequency instability thus is the crudest way to get both a fairly accurate thermodynamic description and melting of a solid without, however, a qualitatively correct singlet distribution function. A similarly successful model in three dimensions has not yet been found; the straightforward extension of the correlated cell model fails to predict a first-order melting transition.

The conclusion that the singlet distribution function is sensitive to the low-frequency phonons was deduced previously<sup>33</sup> from the elastic theory of solids, which should be accurate for long wavelengths. In fact, the singlet distribution function could be shown, due to these long wavelength modes, to have a half-width which becomes unbounded as the number of particles increases indefinitely in two-dimensional systems. In three-dimensional systems the half-width is bounded, and within the elastic theory each mode contributes equally to the second moment of the singlet distribution function. Therefore in three dimensions the singlet distribution in the solid phase is qualitatively different from the one in the fluid phase, where it is a constant. Inasmuch as this distinction, however, does not apply to the two-dimensional fluid and solid, the feature distinguishing between these two states of matter is best described theoretically by sticking to the previous point of view that a solid as opposed to a fluid can support a transverse wave. The lack of spacial localization in the two-dimensional systems indicates that a sufficient condition for the existence of a solid merely involves relative ordering of the particles.

Previous theoretical ways of accounting for melting of hard spheres from integral equations have been notoriously unreliable.<sup>34</sup> Most integral equations either give no indication of melting, or, predict it to occur at unphysical densities.<sup>35</sup> The one integral equation which originally led to the suggestion of melting<sup>18</sup> for hard spheres also shows the melting singularity in one dimension,<sup>□</sup> where it can be proven that no phase transition occurs. Lattice theories also have serious difficulties in describing melting in spite of their success in accounting for the vaporization process. This is because the melting density is so high and hence the accessible configurational phase space so complex and tenuously connected that it is no longer adequate to estimate its volume by a coarse grid.<sup>36</sup> On the other hand, at the critical density, which is much lower, this coarse network is reasonably adequate. Because at the melting point it is necessary to use a much finer mesh (interactions extend over many lattice sites), the primary advantage of the lattice model is lost, namely, it is no longer possible to evaluate the model analytically. Furthermore, it must be expected and indeed it has been confirmed that extraneous, unphysical discontinuities<sup>37</sup> will be found as the mesh size is varied until the grid is fine enough to estimate the phase volume well.

The computer experiments are of course, not rigorous proof of the existence of the hard sphere melting transition. They must be regarded only as a very suggestive indication, and judged on the basis of how this behavior would be reproduced by infinite systems. For this purpose the dependence of the phase transition behavior on the number of particles was studied. An analysis of the pressure at the transition shows that it shifts with the number of particles,  $N$ , as the  $N$ -particle communal entropy.<sup>38</sup> This means that the predominant number-dependent correction necessary to extrapolate to the transition pressure for macroscopic system is simply the entropy difference

between  $N$  particles confined to a cell and an infinite number at the same density. The usual cell theories, referred to previously, confine one particle per cell, and their one-particle communal entropy has often been cited as the origin of the melting entropy. This, however, is not at all correct, in spite of the fact that in the solid a distinct particle is confined to a cell and in the fluid the entire volume of the container is accessible to every particle. The communal entropy does appear somewhere between the perfect gas and the close-packed solid, but only gradually.<sup>20,38</sup> A calculation shows that only a small fraction of it appears across the melting transition, (see Fig. 5).

Another way to study the number dependence of the computer results is to see how they extrapolate to the behavior of an actual macroscopic system. Comparison with Lindemann's law, cited already, suggests that such an extrapolated equation of state will agree well with experiment. Indeed, choosing an interatomic potential which fits an isotherm for argon in both the pure solid and the pure liquid phase at densities removed from the melting condition leads to predictions of melting on the computer<sup>39</sup> in close correspondence to the argon melting line.

In this comparison with experiment, the intermolecular potential cannot, of course, be strictly considered as having a hard core. The question hence arises as to whether any soft repulsive potential by itself would still lead to melting. The softest core that one can conceive of, is the one obtained at extremely high temperatures and pressures where the nuclei repel each other by a Coulomb force law, and where all the electrons can be considered, because of their high zero point energy, to form a uniform background. The problem is then whether, under the conditions similar to those found in the interior of white dwarf stars, a solid is still formed and hence whether

there would practically ever be a solid-liquid critical point analogous to the liquid-gas one. The location of a melting transition for this purely repulsive Coulomb gas<sup>40</sup> not only indicates the absence of a fluid-solid critical point for it, but also for any other substance, since all repulsive potentials lie in between the two extremes of the hard sphere and Coulomb repulsions. The melting transition for the purely Coulombic repulsive potential is in poorer agreement with Lindemann's law, as might be expected, since this very soft repulsive potential blurs the geometric aspects of melting.

## V. THE HIGH DENSITY REGION

Although the high density or solid region is not the proper subject of discussion in a book devoted to fluids, it is worthwhile to make a few brief remarks to amplify the previous description of fluids and melting. The first remark concerns consideration of the van der Waals' model as possibly a more accurate description of a high temperature solid near its melting point than the customary harmonic oscillator model. The question of which one is the more accurate depends on the importance of harmonic forces in any real situation. The van der Waals' approximation is diametrically opposed to the harmonic oscillator approximation in that it represents the completely anharmonic extreme. From the point of view of representing an asymptotic limit, as well as containing melting, the consequences of the van der Waals' model should be and have been partially worked out in the solid phase.

The limit in this model equivalent to the low temperature harmonic oscillator limit is the close-packed one, since in either case the particles are completely localized at their lattice position and hence the usual cell theories give the exact equation of state.<sup>6</sup> The properties at densities

slightly lower than the close-packed density should be expressible in a power series in the free volume<sup>31</sup> (volume of the container less the volume occupied by the particles themselves,  $v-v_0$ ). Accordingly,

$$pV/NkT = D/\alpha + c_0 + c_1\alpha + c_2\alpha^2 + \dots ,$$

where  $\alpha = (v-v_0)/v_0$  and  $D$  is the number of dimensions. The first term on the righthand side is the one that can be proven to be asymptotically exact in the limit of close packing ( $\alpha \rightarrow 0$ ). However, unlike the low density region, where a power series in  $1/\alpha$  can be shown to exist, and where the coefficients in this virial expansion can be theoretically evaluated, at high density no such theory exists. The coefficients,  $c$ , have however, been obtained empirically on the computer; they are given in Table II. These coefficients are compared to the ones given by the usual cell theory and the correlated cell theory. The accurate agreement with the correlated cell theory indicates that this model is nearly quantitative in the solid phase.

An equivalent expansion about the close-packed limit can be carried out in three dimensions for spheres either about the face-centered or the hexagonal close-packed structure. An effort to detect a difference in the solid equations of state failed within the accuracy of the numerical method, which was about 0.01%. This result is not unexpected in view of the previous remarks on the importance of various wavelength modes to the thermodynamic properties. Since these two close-packed structures have the same arrangement of first and second nearest neighbors as well as the same overall density, not only the low-frequency, but, more significantly, the high-frequency spectra as well must be the same. Hence, since only the intermediate frequency spectrum differs between the two structures, their thermodynamic properties cannot differ very much. The lack of importance of the low frequency spectrum to the thermodynamic properties is shown by the small dependence of thermodynamic

properties on the number of particles used in the machine calculations.<sup>37</sup>

In the larger systems primarily the low-frequency spectrum is changed inasmuch as longer wavelength fluctuations are possible, while the high-frequency spectrum is unaltered from smaller systems. Then, as long as systems of more than 100 particles are studied, the number dependence of the results is hardly detectable.

For very precise thermodynamic results it is, of course, necessary to take correlated longer wavelength motions into account. This shows up clearly in the entropy calculation in the close-packed limit, which, unlike the equation of state, is not correctly given by the cell theory. The reason for this is that the functional form of the partition function must be of the free volume type but the coefficient multiplying the free volume, that is the absolute value of the free volume, is unknown. Hence a derivative of the logarithm of the partition function, that is, for example, the pressure, is given exactly while the entropy is not. Since the absolute value of the free volume depends on the extent of correlated motions, the entropy is in turn a measure of that motion. Even though the entropy is not exactly calculated by the cell theory, it again must be emphasized that the entropy at close-packing<sup>41</sup> is remarkably accurate. It is obtained by integrating the machine determined equation of state all the way from the perfect gas state across the melting transition to close-packing. Even in the one-dimensional hard rod system where correlated motion play a relatively more important role, and where hence the biggest error in the cell theory estimate of the entropy at close-packing occurs, it can be exactly calculated to be only  $0.3 Nk$ . The error is largest for that system, because in one-dimension particles are least localized by their neighbors. Thus it does not require as improbable an event as in two or three dimensions to set up a long wavelength fluctuation. In two and three dimensions the entropy at

close-packing as calculated by the one-particle cell theory is in error by about 0.1 Nk. There is some uncertainty (of the order of 0.05 Nk) in this estimate due to the uncertainty of where to locate the liquid-solid tie line. To account for this entropy by taking larger and larger cells into consideration seems a slowly converging process.<sup>41</sup> Although little entropy is carried by the lower frequency modes, it is necessary to go to cells of the order of 100 particles to account for the 0.1 Nk carried by them in entropy, as the number dependence of the machine calculations shows. It would have been nice to have an exact theory for the entropy at close-packing since then the tie line between the solid and fluid branch of the equation of state determined by molecular-dynamics could have been drawn on thermodynamic grounds.

## VI. THE LOW-DENSITY REGION

In the low-density region where the energy density fluctuates and collisions involving small clusters of particles predominate, van der Waals' mean-field theory is not applicable. Fortunately, the exact virial series theory is available in that region.<sup>7</sup> The virial coefficients,  $B_n$ , in the series expansion of the compressibility factor

$$pV/NKT = 1 + B_2(N/V) + B_3(N/V)^2 + B_4(N/V)^3 + \dots ,$$

can describe a dense gas accurately if a sufficient number of terms in the series is used. Recently the seventh virial coefficient for hard spheres was calculated, using Monte Carlo integration.<sup>9</sup> The resulting seven-term series agrees with the molecular-dynamic equation of state, within the latter's 1% accuracy, up to half the close-packed density. At higher densities (the hard-sphere fluid phase is stable up to about two-thirds the close-packed density) the truncated series lies below the dynamic results by as much as

10%, as can be seen in Fig. 6.

A popular game is to extend the useful region of the virial or other series by representing it as a quotient of two polynomials. The coefficients in the polynomials are so chosen that the series expansion of the quotients reproduces the known coefficients in the represented series. An example of this polynomial representation, called a Padé approximant, is

$$pV/NkT = \frac{1 + 0.554683x + 0.019716x^2 + 0.018105x^3}{1 - 0.445317x - 0.316972x^2 + 0.151085x^3},$$

where  $x$  is  $B_2(N/V)$ . The series expansion of this expression reproduces the first seven hard-disk virial coefficients. It is obvious that many different Padé approximants can be constructed<sup>9</sup> by varying the number of terms in the numerator and denominator. These different possibilities do not always agree well with one another. Thus, for example, approximants of the type represented above, which reproduce only six terms of the hard-sphere virial series<sup>42</sup>, generally agree better with the machine-generated equation of state than do the approximants that reproduce all seven known terms. For the seven-term virial series the Padé approximant to another function involving the equation of state was found to be more accurate:

$$(pV/NkT)(1-\rho) = \frac{1 + \sum_{i=1}^I c_i \rho^i}{1 + \sum_{j=1}^J c_j \rho^j},$$

where  $\rho = v_0/v$ . Figure 6 shows that not only is this form more accurate but also that the results do not depend so much on the number of terms used, that is on the combination of  $I$  and  $J$  used to fit the first  $(I+J+1)$  virial coefficients. This can be seen from Fig. 6 where the  $I, J$  combinations 2,2; 3,1; 3,2; 4,2; and 3,3, which reproduce 5, 6, or 7 virial coefficients, all

lie within the width of the curve. Thus as a practical suggestion the least sensitive form of a Padé approximant to a function is likely to be the best one to use.

Machine calculation of higher virial coefficients is not a particularly fast or easy way to generate numerical equations of state. The evaluation of the seventh hard-sphere virial coefficient took weeks of computer program writing as well as 25 hours of CDC 3600 computer time. In a comparable amount of time it is possible to generate 5 high-density equation of state points, within an accuracy of 1%, using either the molecular dynamic or the Monte Carlo method.

The evaluation of the seventh virial coefficient represents about the present practical limit of numerical work. The reason is that the number of integrals<sup>43</sup> contributing to the  $n$ th virial coefficient is about  $2^{\binom{n}{2}}/n!$ , which is over 6000 for  $n$  equals 8. The bookkeeping problem of classifying and operating on all of these graphs forms in itself a major part of the task. It is chiefly this cumbersome classification problem<sup>44</sup> which has so far prevented the evaluation of the 8th and higher terms in those simplified models where the integrals themselves are relatively easy to evaluate.<sup>45,46</sup> The classification problem for the seventh virial coefficient is already quite time-consuming, and accounted for a good deal of the slowness associated with the Monte Carlo hard-sphere calculation. For more general potentials, however, the calculation of the multidimensional integrals themselves represents a much more severe problem than the bookkeeping one. Here the computer can be of great help by utilizing Monte Carlo techniques. The hard-sphere potential is especially favorable for Monte Carlo application, because all the contributing regions of configuration space have the same weight. In the presence of an attractive potential it is necessary for the evaluation of the higher virial

coefficients to introduce importance-sampling methods; that is sampling the configuration space regions most often which contribute the largest part to the integral. This procedure is analogous to the modified Monte Carlo method<sup>47</sup> used to generate configuration-space averages. The transition probabilities in a Markov chain leading to the evaluation of virial coefficients would involve Mayer f-functions rather than Boltzmann factors. Even for hard spheres, where the integrals were evaluated not by a Markov chain but by the simpler, completely random sampling method, an obstacle to numerical accuracy was encountered because of the near cancellation of positive and negative integrals in their contributions to the virial coefficient. It was hence found expedient to reformulate Mayer's original way of calculating virial coefficients to avoid much of this cancellation.<sup>48</sup> The remainder of this section is devoted to describing this reformulation in detail.

In Mayer's expressions for the virial coefficients the integration variables are the particle coordinates while the integrands, which depend explicitly on the potential function,  $\phi(\mathbf{r}_i - \mathbf{r}_j)$ , are products of Mayer f-functions,  $f_{ij} \equiv \exp[-\phi(\mathbf{r}_i - \mathbf{r}_j)/kT] - 1$ . In the nth virial coefficient all different products of f-functions occur which link the n particles together.<sup>7</sup> Because f is zero beyond the range of the interparticle forces, the integrand vanishes unless all n particles are close together, hence the name cluster integrals. For the hard-sphere example each f-function is -1 if the particles linked by it overlap, and zero otherwise.

A pictorial representation of the integrals as "star graphs", using lines to represent f-functions linking the particles (points in the graphs) together, was introduced by Mayer and has been adopted universally as a convenient and compact shorthand notation. The virial coefficients through  $B_5$  have the following form in this notation:

$$B_2 = -\frac{1}{2} \int_{-\infty}^{\infty} \int_{-\infty}^{\infty} \int_{-\infty}^{\infty} [\exp(-\phi_{12}/kT) - 1] dx_2 dy_2 dz_2 \equiv -\frac{1}{2} \int [c - c] d\vec{r}_2 ;$$

$$B_3 = -\frac{1}{3} \iint [ \text{triangle} ] d\vec{r}_2 d\vec{r}_3 ;$$

$$B_4 = -\frac{1}{8} \iiint [ 3 \text{square} + 6 \text{diag1} + \text{diag2} ] d\vec{r}_2 d\vec{r}_3 d\vec{r}_4 ;$$

$$B_5 = -\frac{1}{30} \iiint \iiint [ 12 \text{pentagon} + 60 \text{diag3} + 10 \text{diag4} + 10 \text{diag5} + 60 \text{diag6} + 30 \text{diag7} + 30 \text{diag8} + 15 \text{diag9} + 10 \text{diag10} + \text{diag11} ] d\vec{r}_2 d\vec{r}_3 d\vec{r}_4 d\vec{r}_5 .$$

In writing these expressions contributions from topologically equivalent graphs are grouped together; that is,  $3 \text{square}$  replaces  $\text{square} + \text{diag1} + \text{diag2}$ , for example. Only  $n-1$  particle coordinates appear as integration variables because the cluster integrals are independent of the location of the cluster.

The cancellation of the Mayer integrals for the hard-sphere fifth virial coefficient, for example, is illustrated by pointing out that five of the ten integrals are positive, the other five negative.<sup>42,49</sup> An error of 1% in each individual integral could lead to an error of over 50% in the final coefficient. The high dimensionality of the integrals then represents a problem because so many grid points are required for accurate numerical evaluation. If the integration were carried out in a straightforward manner, a grid for an  $n$ -particle numerical integration based on ten different values of each coordinate, would require  $10^{3n-3}$  points in the grid. Even for  $n$  as small as five this size grid is too large for present computers. Instead the use of the Monte Carlo integration allows the higher dimensional integrals to be evaluated more efficiently. Furthermore, reformulation of the virial series helps overcome the effects of cancellation and thereby improves the accuracy of the results.

The reformulation is carried out by observing that many of the inter-particle distances are not restricted by f-functions. A restriction can be imposed by introducing the function  $\tilde{f} \equiv \exp(-\phi/kT)$ , which is 1 for non-overlapping spheres and zero for overlapping spheres. If the identity  $\tilde{f} + (-f) = 1$  is arbitrarily introduced for each pair of particles not connected by f-functions, graphs with two kinds of lines - the new function,  $\tilde{f}$ , is indicated by a wiggly line - in which all distances are specified, are generated by multiplying out all the factors of  $[\tilde{f} + (-f)]$ . When this is done the unexpected result is that about half of the integrals vanish altogether. The reformulated expressions for  $B_4$  and  $B_5$ , in terms of these "modified star integrals", are

$$B_4 = -\frac{1}{8} \iiint [-2 \text{ (complete-star)} + 3 \text{ (modified star)}] dr_2 dr_3 dr_4 ;$$

$$B_5 = -\frac{1}{30} \iiiii [-6 \text{ (complete-star)} + 45 \text{ (modified star)} - 60 \text{ (modified star)} + 10 \text{ (modified star)} + 12 \text{ (modified star)}]$$

$$dr_2 dr_3 dr_4 dr_5 .$$

Besides being less numerous, the modified star integrals also vary greatly in magnitude whereas the Mayer integrals are all of the same order of magnitude. For one-dimensional hard rods all but one of the integrals contributing to each virial coefficient are zero. The non-vanishing integral is the first one shown in the above expressions for  $B_4$  and  $B_5$ ; it contains no  $\tilde{f}$ -functions and is called the "complete-star" integral. The complete-star integral in one, two, and three dimensions now makes the largest contribution to  $B_n$  through at least the seventh virial coefficient, while in the Mayer f-function formulation this same integral was the smallest contributor. All integrals involving the f-functions are smaller than the smallest Mayer integral. This shows that cancellation is a less serious problem in the reformulated expression.

All star integrals, with  $f$ -functions, or modified star integrals, with  $f$  and  $\tilde{f}$ -functions, can be calculated by a straightforward "Monte Carlo" procedure, as illustrated by the evaluation of  $\iint f_{12}f_{13}f_{23}dx_2dx_3$  for one-dimensional hard rods of length  $\sigma$ . Because the integrand is  $(-1)^3$  when all three pairs of rods overlap, and zero otherwise, the integral is  $(-1)$  times the (two-dimensional) volume of configuration space in which all three rods overlap. Random configurations in a somewhat larger volume of configuration space, corresponding to the overlaps of pairs 12 and 23, with 13 not specified, can easily be generated. Particle 1 is placed, for convenience, at the origin. Then random numbers distributed uniformly from  $-\sigma$  to  $+\sigma$  can be used to place particle 2 so that these two particles overlap. Particle 3 can then be placed anywhere between  $x_2-\sigma$  and  $x_2+\sigma$  so that  $f_{23}$  is also  $-1$ . The diamond-shaped region of 3-particle configuration space corresponding to these conditions is outlined in Fig. 7. The fraction of configurations in which  $f_{13}$  is also  $-1$  (configurations in the shaded hexagonal region of Fig. 7) is then tabulated. The ratio of the shaded to the total area is an estimate for the ratio of the two integrals:

$$\frac{-\iint f_{12}f_{13}f_{23}dx_2dx_3}{\iint f_{12}f_{13}dx_2dx_3} = \frac{-\iint [\text{Diagram}]dr_2dr_3}{-\iint [\text{Diagram}]dr_2dr_3}$$

From the Monte Carlo estimate of the ratio and the known value of the denominator,  $4\sigma^2$ , the numerator can be calculated. This same principle has been used to calculate the hard-sphere integrals contributing to  $B_5$ ,  $B_6$ , and  $B_7$ .

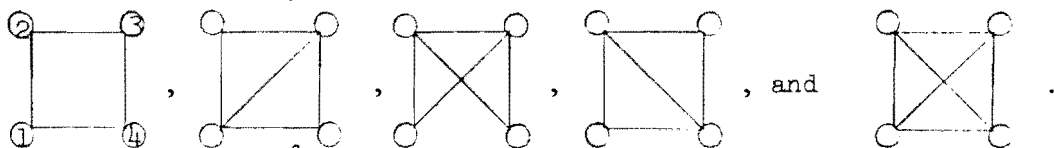
Because each integral contributing to  $B_5$  involves at least the  $f$ -functions  $f_{12}f_{23}f_{34}f_{45}$ , each integral is a part of the volume in the 12-dimensional configuration space for which  $|r_{12}|$ ,  $|r_{23}|$ ,  $|r_{34}|$ , and  $|r_{45}|$  are less than the hard-sphere diameter,  $\sigma$ . Random configurations are thus generated which satisfy  $f_{12} = f_{23} = f_{34} = f_{45} = -1$ , and subsequently the fraction of total configurations satisfying the restrictions imposed by the additional  $f$  and  $\tilde{f}$ -functions

are tabulated. For example, the ratio

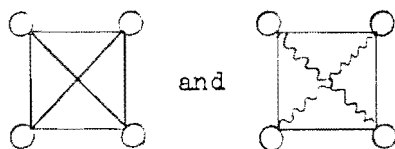
$$\int \int \int \int \int \left[ \begin{array}{c} \textcircled{3} \\ \textcircled{2} \text{---} \textcircled{4} \\ \textcircled{1} \text{---} \textcircled{5} \end{array} \right] dr_2 dr_3 dr_4 dr_5 / \int \int \int \int \int \left[ \begin{array}{c} \textcircled{3} \\ \textcircled{2} \text{---} \textcircled{4} \\ \textcircled{1} \text{---} \textcircled{5} \end{array} \right] dr_2 dr_3 dr_4 dr_5$$

equals the fraction of configurations with  $|r_{15}|$  less than  $\sigma$  and  $|r_{13}|$ ,  $|r_{14}|$ ,  $|r_{24}|$ ,  $|r_{25}|$ , and  $|r_{35}|$  greater than  $\sigma$ . The errors in Monte Carlo integration can be estimated accurately from the statistical fluctuations since the relative error in the values of the integrals is inversely proportional to the square root of the number of trials. It is clear that long runs are needed to obtain four or five significant figures. The present values of the first seven virial coefficients for disks and spheres are given in Table II. The statistical errors in the 1953 Monte Carlo calculations<sup>47</sup> of  $B_5$  for hard spheres and hard disks were estimated to be  $\pm 5\%$ . Later more accurate calculations<sup>42,49</sup> showed that the errors were  $+4\%$  for spheres and  $-6\%$  for disks. The simplicity and accuracy of error estimates is an advantage of Monte Carlo integration over alternative techniques based on truncating series expansions of the integrands.

To give a concrete example of the advantage of the  $f$  recipe over Mayer's recipe for numerical virial coefficient calculations, consider the calculation of  $B_4$  for hard spheres, using random configurations with the overlap restrictions  $f_{12} = f_{23} = f_{34} = -1$ . The various Mayer stars that can be generated from this starting condition are



while in the reformulated  $f$  calculations only those configurations contributing to



are tabulated. The  $f$ -function expression for  $B_4$  has the form

$$B_4(f) = -\frac{1}{8} \iiint [3 \text{ (square)} + 2 \{ \text{diag 1} + \text{diag 2} + \text{diag 3} \} + \text{diag 4}] dr_2 dr_3 dr_4 .$$

Expressing each of the integrals in this expression in terms of wiggly-line integrals, gives the result

$$B_4(f) = -\frac{1}{8} \iiint [3 \text{ (wiggly square)} + \{ -\text{diag 1} + 2 \text{diag 2} - \text{diag 3} \} - 2 \text{diag 4}] dr_2 dr_3 dr_4$$

By rewriting the f-function results one finds that the calculation includes a sum of three terms, shown in curly brackets, which is known to be exactly zero. The error associated with this unnecessary work is eliminated by using the reformulated version.

TABLE I

Values of the van der Waals constant as a function of density for a square-well potential

$v/v_0$	$a_1^*(1.5)$	$a_2(1.5)$	$a_1(1.8)$
$\infty$	7.04	7.04	14.31
7.0	8.06	9.11	15.44
4.0	8.82	10.43	15.98
3.0	9.31	11.09	16.18
2.5	9.63	11.26	--
2.0	9.91	10.65	15.85
1.7	9.91	8.95	15.23
1.6	9.82	7.85	14.87
1.42	9.40		
1.35	9.09		
1.00	9.00		

\*The number in parenthesis indicates the range of the potential.

$$a_1(1.5) = 7.035 + \frac{7.273}{v/v_0} + \frac{1.249}{(v/v_0)^2} - \frac{6.087}{(v/v_0)^3} - \frac{4.976}{(v/v_0)^4} \quad v/v_0 > 1.6$$

$$a_2 = a_1 - (v/v_0) \frac{\partial a_1}{\partial (v/v_0)}$$

$$a_1(1.8) = 14.312 + \frac{9.145}{v/v_0} - \frac{7.452}{(v/v_0)^2} + \frac{9.774}{(v/v_0)^3} + \frac{0.889}{(v/v_0)^4} \quad v/v_0 > 1.6$$

$a_1$  and  $a_2$  in units of  $a/\epsilon v_0$ , where  $\epsilon$  is the depth of the potential.

TABLE II

High density expansion coefficients of the compressibility factor  $pV/NkT$ , for disks.

	$c_0$	$c_1$	$c_2$
Molecular dynamics	1.89	0.8	> 0
Cell theory	1.56	-0.1	> 0
Correlated cell theory	1.89	0.8	> 0

TABLE III

The virial coefficients for hard spheres and disks<sup>(a)</sup>

	$B_2/b$	$B_3/b^2$	$B_4/b^3$	$B_5/b^4$	$B_6/b^5$	$B_7/b^6$
spheres	1.0000	0.62500	0.28695	0.1103	0.0386	0.0138
disks	1.0000	0.78200	0.53223	0.3338	0.1992	0.1141

(a)  $b$  is the second virial coefficient:  $\frac{1}{2} \pi \sigma^2$  for disks and  $\frac{2}{3} \pi \sigma^3$  for spheres.

Fig. 1 The compressibility factor versus the reciprocal temperature (reduced by the potential depth) for a square-well potential of a range 50% larger than the hard core diameter at  $v/v_0$  of 2. The heavy curve with the circles represents the computer data, while the light line represents the theoretically calculated high temperature slope.

Fig. 2 The compressibility factor versus the reciprocal temperature (degrees Kelvin) for argon at 35.7 cc. The circles represent experimental data and the two straight lines are drawn as the slope of the curve at the two extremes of the temperature range. The change of collision diameter with temperature is illustrated in that the lower temperature intercept corresponds to a diameter of  $3.15 \text{ \AA}$  while the high temperature one corresponds to  $3.06 \text{ \AA}$ .

Fig. 3 The free path distribution for a square-well potential at reduced temperatures of 1.4 and 0.6 divided by the free path distribution for hard spheres at the same  $v/v_0$  of 1.6 vs. the free path length measured in terms of the kinetic mean free path,  $\lambda_0$ . The  $T^*$  of 1.4 curve is nearly in agreement with the van der Waals' theory prediction of a horizontal line at one, while the  $T^* = 0.6$  is in remarkable agreement with the simple hard sphere kinetic theory prediction (dashed line). This Figure is taken from Ref. 23.

Fig. 4 The probability of an excursion of a hard disk from its lattice site at  $A/A_0$  of 1.26 in an 870 particle system after 2,000,000 collisions as a function of radial distance measured in units of the interparticle distance. The curve refers to a directional cone with an apex of one degree width pointed directly at the center of a neighboring particle. The circles refer also to a wedge of one degree but pointed 15 degrees away from a line joining the two neighbors while the one degree wedge represented by crosses points  $30^\circ$  away from a line joining the two neighbors which means that it points exactly

in between two nearest neighbors to the central particle. The curve to the left of the dotted line is the same for all these various one degree slices. The ones to the right of the dotted line are continued but drawn with a 100 times larger scale so as to see greater detail. The peak at an interatomic distance in the curve and the lack of one in the wedge represented by the crosses indicates sliding in directions of lines of atoms.

Fig. 5 The solid and fluid branches of the hard sphere equation of state. The horizontal line is a guess at the tie line connecting the two phases and the dotted extensions of the solid and fluid branches represent metastable states generated on the computer. The area of the rectangle bounded by the two vertical lines at the ends of the tie line is then a measure of the entropy of melting. The communal entropy of melting is approximately equal to the hatched area, namely the difference between the entropy of melting and the entropy if the system had remained a solid. It can be seen that the communal entropy change is only a small fraction of the entropy of melting.

Fig. 6 The equation of state for a hard sphere fluid. The solid curve widens at high density to cover the range of values calculated using 5, 6, and 7 virial coefficients Padé approximants to  $pV/NkT(1-\rho)$ . The open circles represent molecular dynamic results. Values of  $pV/NkT$  calculated from the truncated virial series of 1 through 7 terms at  $2/3$  of the close-packed density are indicated by the filled circles labeled 1 through 7 near the righthand side of the figure.

Fig. 7 Configuration space for three hard rods of length  $\sigma$ . The coordinates of particles 2 and 3 are measured relative to that of particle 1, which is at the origin. In the outlined area  $f_{12} f_{23}$  is non-vanishing; in the hexagonal area  $f_{12} f_{23} f_{13}$  is non-vanishing.

REFERENCES

- <sup>1</sup>M. Ross and B.J. Alder, to be published, J. Chem. Phys.
- <sup>2</sup>E.A. Guggenheim and M.L. McGlashan, Proc. Roy. Soc. (London) A255, 456 (1960).
- <sup>3</sup>"Molecular Theory of Gases and Liquids", J.O. Hirschfelder, C.F. Curtiss, and R.B. Bird, John Wiley & Sons, Inc., New York (1954).
- <sup>4</sup>E.B. Smith and B.J. Alder, J. Chem. Phys. 30, 1190 (1959).
- <sup>5</sup>"Lattice Theories of the Liquid State", J.A. Barker, The MacMillan Co., New York (1963).
- <sup>6</sup>Z.W. Salsburg and W.W. Wood, J. Chem. Phys. 37, 798 (1962).
- <sup>7</sup>"Statistical Mechanics", J.E. Mayer and M.G. Mayer, John Wiley & Sons, Inc., New York (1940).
- <sup>8</sup>J.L. Lebowitz and O. Penrose, J. Math. Phys. 5, 841 (1964).
- <sup>9</sup>F.H. Ree and W.G. Hoover, to be published, J. Chem. Phys.
- <sup>10</sup>B.J. Alder, Phys. Rev. Letters 12, 317 (1964).
- <sup>11</sup>H. Eyring and T. Ree, Proc. Natl. Acad. Sci. 47, 526 (1961).
- <sup>12</sup>A. Eisenstein and N.S. Gingrich, Phys. Rev. 62, 261 (1942).
- <sup>13</sup>A.V. Grosse, Science 147, 1438 (1965).
- <sup>14</sup>J.D. van der Waals, Over de continuïteit Vanden gas-en vloeïstoftoestand (Dissertation, Leiden, 1873).
- <sup>15</sup>D. Enskog, Archif för Matematik, Astronomi, och Fysik, 15, 16 (1922).
- <sup>16</sup>B.J. Alder and T.E. Wainwright, J. Chem. Phys. 33, 1439 (1960).
- <sup>17</sup>M. Kac, G.E. Uhlenbeck, and P.C. Hemmer, J. Math. Phys. 4, 216 (1963).

References (continued)

- <sup>18</sup>J.G. Kirkwood, V.A. Lewinson, and B.J. Alder, J. Chem. Phys. 20, 929 (1952).
- <sup>19</sup>"Regular Solutions", J.H. Hildebrand (Prentice-Hall, Engelwood Cliffs, N.J., (1962).
- <sup>20</sup>B.J. Alder and T.E. Wainwright, Phys. Rev. 127, 359 (1962).
- <sup>21</sup>K. Kowasaki and I. Oppenheim, Phys. Rev. 139, A1763 (1965).
- <sup>22</sup>"The Statistical Mechanics of Simple Liquids", S.A. Rice and P. Gray, Interscience, New York (1965).
- <sup>23</sup>"Prediction of Transport Properties of Dense Gases and Liquids", B.J. Alder, UCRL-14891-T (1966); T. Einwohner and B. Alder, to be published.
- <sup>24</sup>S. Glasstone, K.J. Laidler, and H. Eyring, The Theory of Rate Processes (McGraw-Hill Book Company, Inc., New York, 1941).
- <sup>25</sup>B.J. Alder and T. Einwohner, J. Chem. Phys. 43, 3399 (1965).
- <sup>26</sup>J.H. Dymond and B.J. Alder, J. Chem. Phys. 45, 2061 (1966).
- <sup>27</sup>B.J. Alder and T.E. Wainwright, Transport Processes in Statistical Mechanics, I. Prigogine (Interscience Publishers, New York) 1958.
- <sup>28</sup>F.A. Lindemann, Physik. Z. 11, 609 (1910).
- <sup>29</sup>J. Rowlinson, Molec. Physics 8, 107 (1964).  
C.H. Longuet-Higgins and B. Widom, Molec. Physics 8, 549 (1964).  
E.A. Guggenheim, Molec. Physics 9, 43 and 199 (1965).
- <sup>30</sup>M. Born, Proc. Cambr. Phil. Soc. 36, 160 (1940).
- <sup>31</sup>B.J. Alder, W.G. Hoover, and T.E. Wainwright, Phys. Rev. Letters 11, 241 (1963).
- <sup>32</sup>R.J. Buehler, R.H. Wentorf, J.O. Hirschfelder, and C.F. Curtiss, J. Chem. Phys. 19, 61 (1951).

References (continued)

- <sup>33</sup>L. Landau and E. Lifshitz, Statistical Physics, Pergamon Press (London) Chap. XV (1958).
- <sup>34</sup>J. Yvon, Actualities Scientifiques et Industriel, Herman et Cie, Paris (1935); M. Born and H.S. Green, Proc. Roy. Soc. (London) A188, 10 (1946).
- <sup>35</sup>E. Thiele, J. Chem. Phys. 39, 474 (1963); M.S. Wertheim, Phys. Rev. Letters 8, 321 (1963), H.N.V. Temperley, Proc. Phys. Soc. 83, 565 (1964) and 84, 339 (1964).
- <sup>36</sup>W.G. Hoover, B.J. Alder and F.H. Ree, J. Chem. Phys. 41, 3258 (1964).
- <sup>37</sup>D.S. Gaunt and M.E. Fisher, J. Chem. Phys. 43, 2840 (1965); L.K. Runnels, Phys. Rev. Letters 15, 581 (1965); A. Bellemans and R.K. Nigam, Phys. Rev. Letters 16, 1038 (1966); F.H. Ree and D.A. Chesnut, to be published, J. Chem. Phys.
- <sup>38</sup>W.G. Hoover and B.J. Alder, to be published, J. Chem. Phys.
- <sup>39</sup>M. Ross and B.J. Alder, Phys. Rev. Letters 16, 1077 (1966).
- <sup>40</sup>S.G. Brush, H.L. Sahlín, and E. Teller, J. Chem. Phys. 45, 2102 (1966).
- <sup>41</sup>W.G. Hoover and B.J. Alder, J. Chem. Phys. 45, 2361 (1966).  
F.H. Stillinger, Z.W. Salsburg, and R.L. Kornegay, J. Chem. Phys. 43, 932 (1965).
- <sup>42</sup>F.H. Ree and W.G. Hoover, J. Chem. Phys. 40, 939 (1964).
- <sup>43</sup>R.J. Riddell and G.E. Uhlenbeck, J. Chem. Phys. 21, 2056 (1953).
- <sup>44</sup>E. Helfand and R.L. Kornegay, Physica 30, 1481 (1964).
- <sup>45</sup>G.E. Uhlenbeck and G.W. Ford in Studies in Statistical Mechanics, edited by J. de Boer and G.E. Uhlenbeck (North Holland Publishing Company, Amsterdam, the Netherlands, 1962), Vol. 1, Part B.
- <sup>46</sup>W.G. Hoover and A.G. De Rocco, J. Chem. Phys. 36, 3141 (1962).

References (continued)

<sup>47</sup>N.Metropolis, A.W. Rosenbluth, M.N. Rosenbluth, A.H. Teller, and E. Teller, J. Chem. Phys. 21, 1087 (1953); M.N. Rosenbluth and A.W. Rosenbluth, J. Chem. Phys. 22, 881 (1954).

<sup>48</sup>F.H. Ree and W.G. Hoover, J. Chem. Phys. 41, 1635 (1964).

<sup>49</sup>S. Katsura and Y. Abe, J. Chem. Phys. 39, 2068 (1963).

□ The precise statement is that the straightforward application of the superposition approximation in triplet space as a product of three pair distribution functions leads to a singularity whether the Born-Green equation is linearized or not. The proper decomposition of the triplet distribution function as a product of a two pair distribution functions leads to the exact result in one dimension.

\* Work performed under the auspices of the U.S. Atomic Energy Commission.

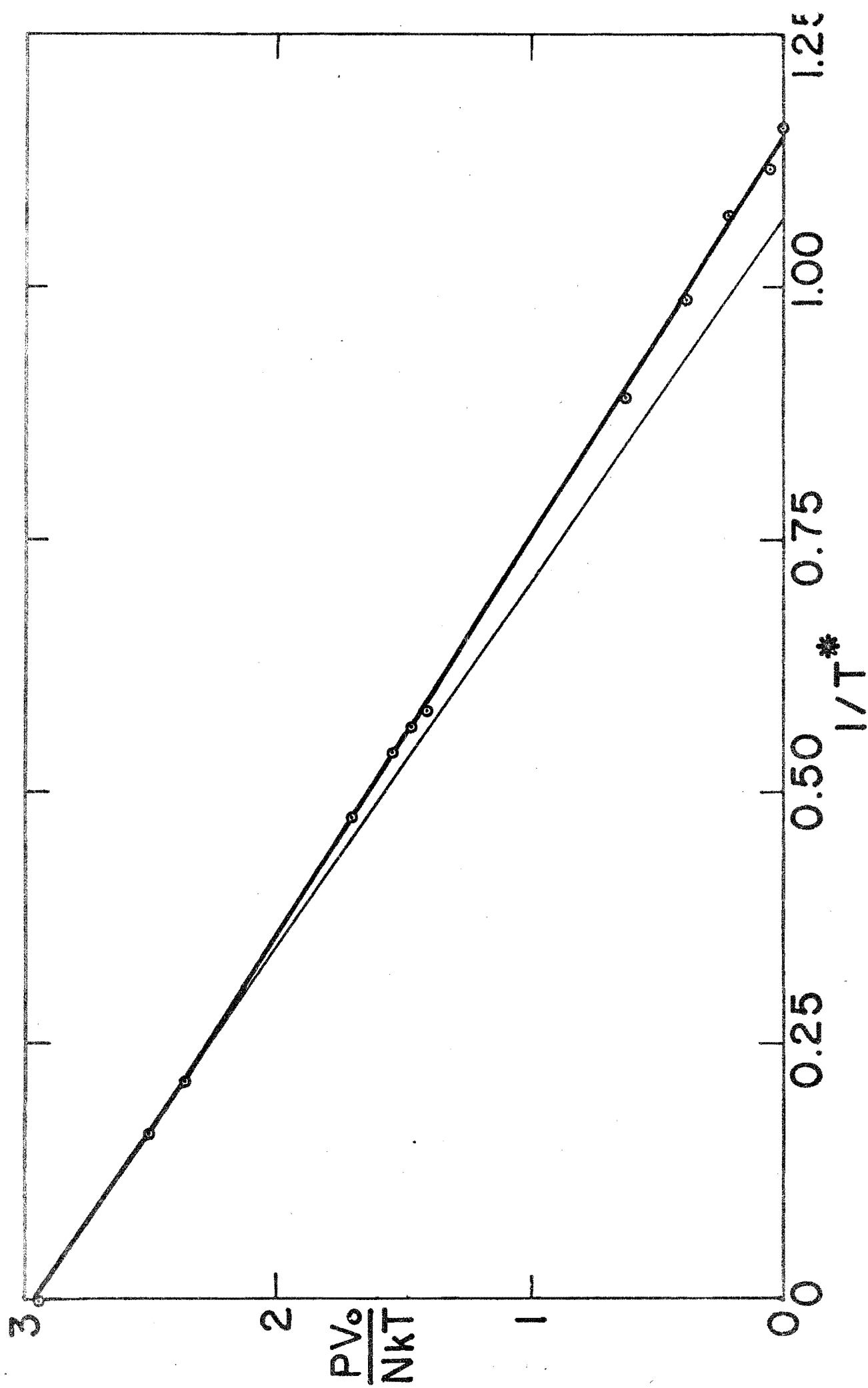
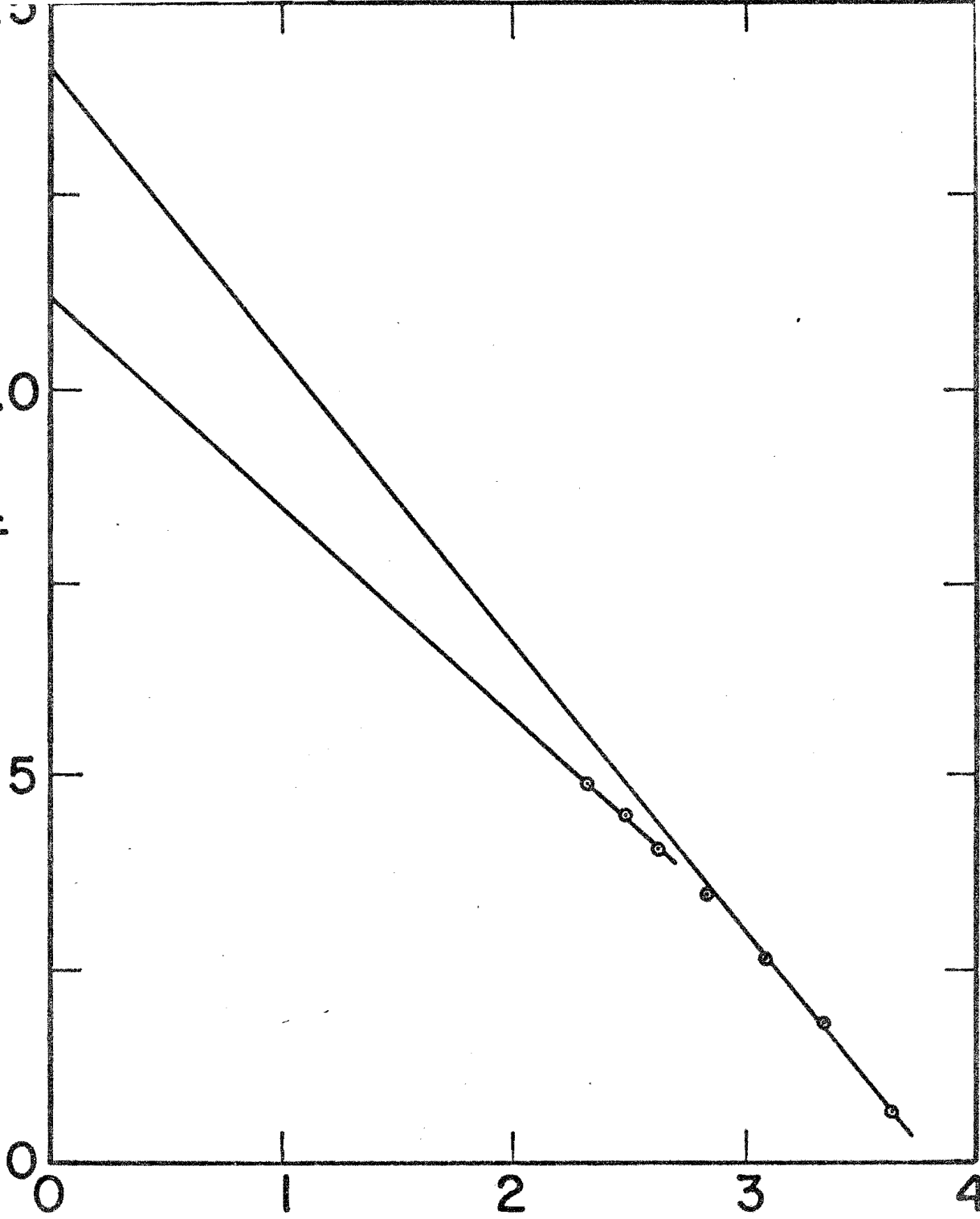


Fig. 1



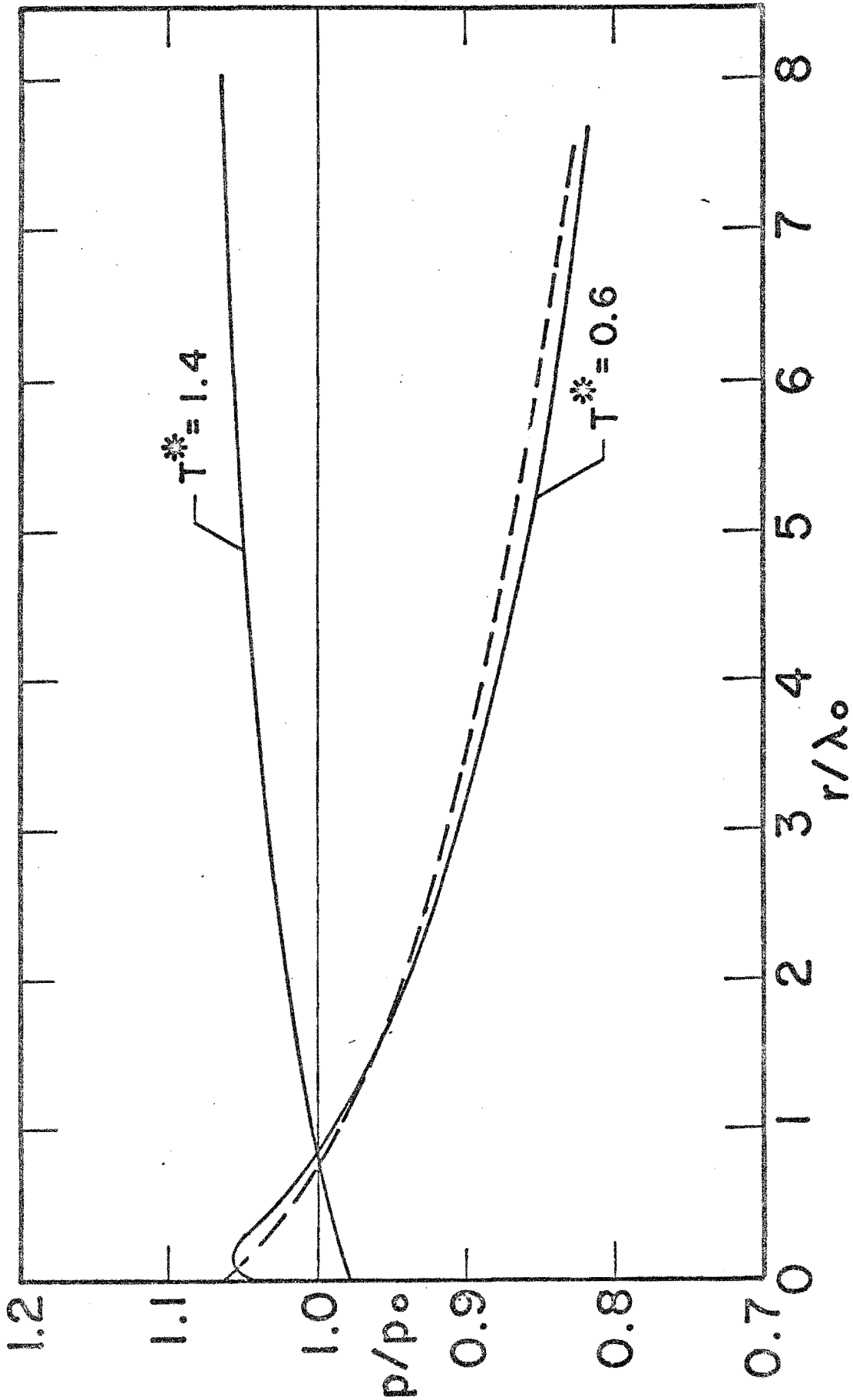
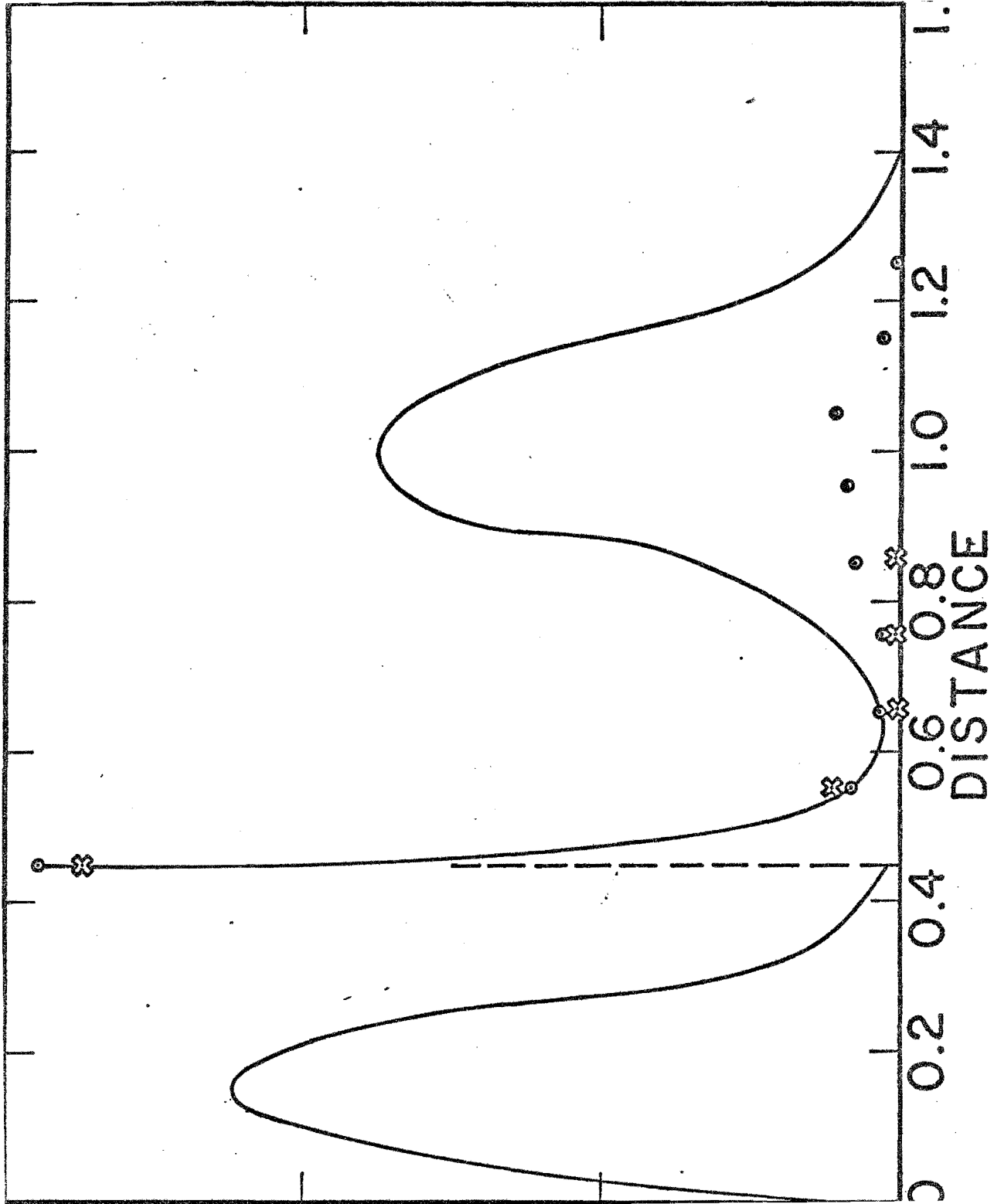
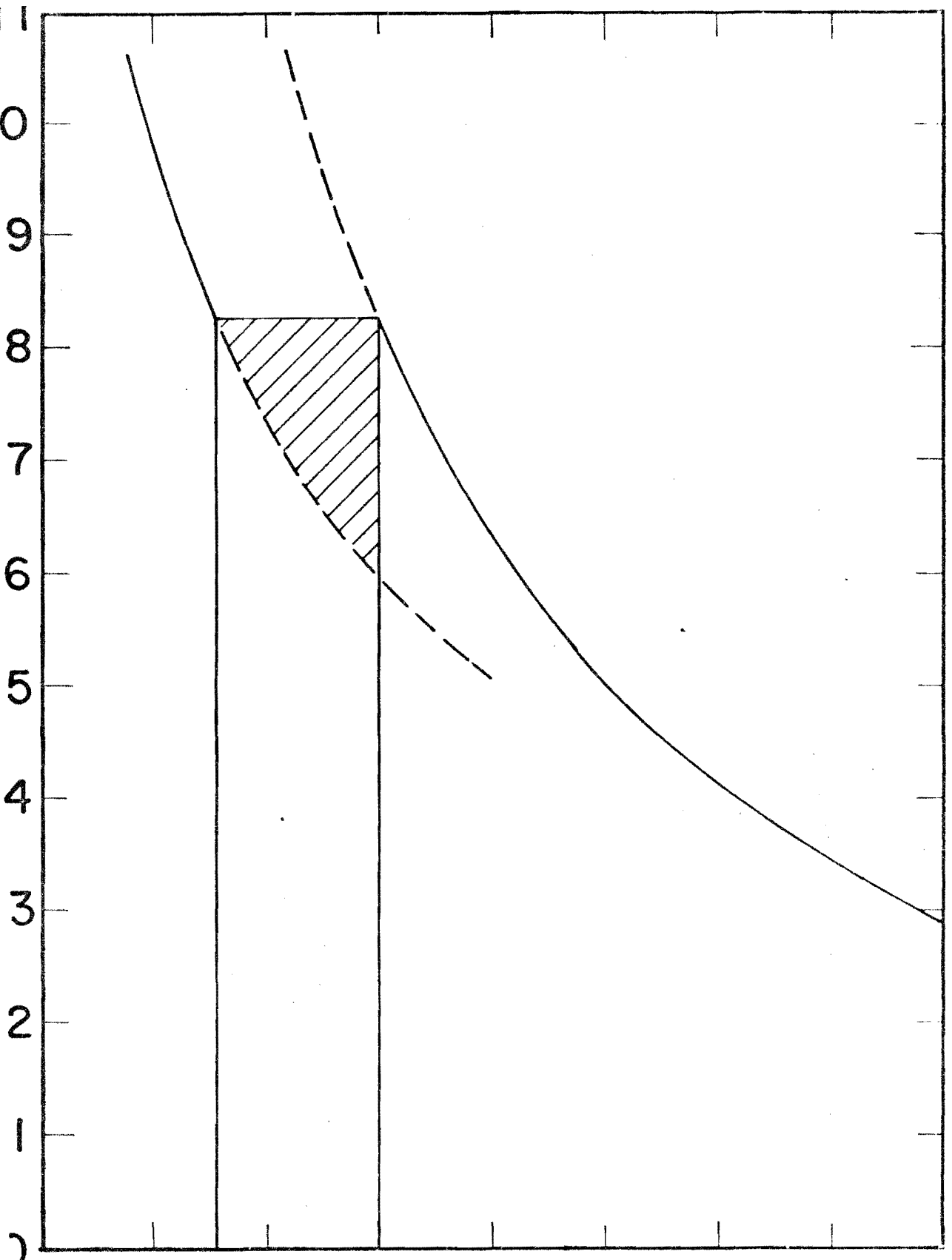


Fig. 3





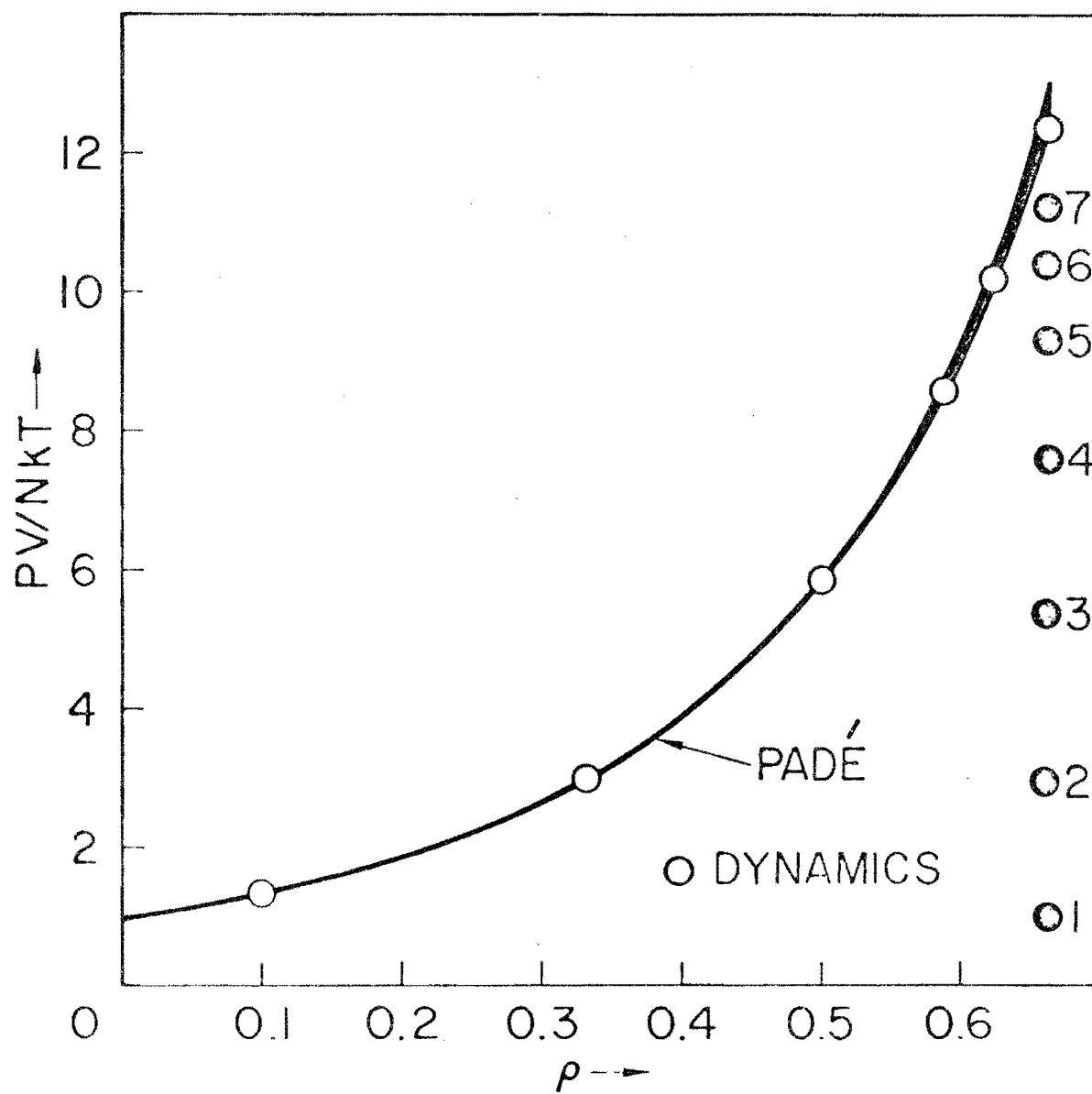


Fig. 6

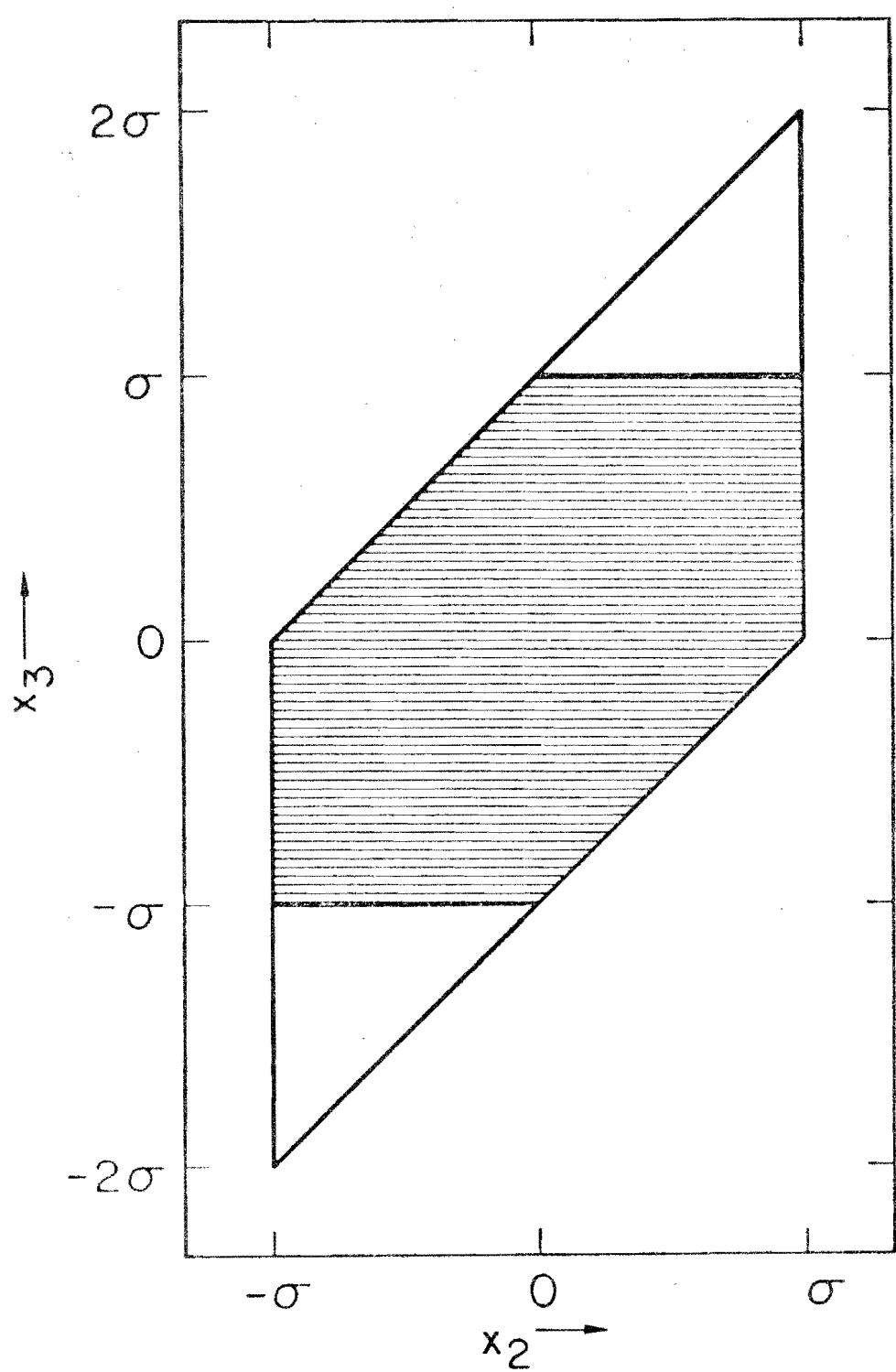


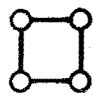
Fig. 7

$$B_2 = -\frac{1}{2} \iiint_{-\infty}^{\infty} [\exp(-\phi_{12}/kT) - 1] dx_2 dy_2 dz_2 \equiv -\frac{1}{2} \int [\text{---} \circ \text{---}] d\vec{r}_2;$$

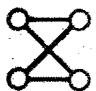
$$B_3 = -\frac{1}{3} \iint [\text{---} \triangle \text{---}] d\vec{r}_2 d\vec{r}_3;$$

$$B_4 = -\frac{1}{8} \iiint [3 \text{---} \square \text{---} + 6 \text{---} \text{---} \text{---} \text{---} + \text{---} \text{---} \text{---} \text{---}] d\vec{r}_2 d\vec{r}_3 d\vec{r}_4;$$

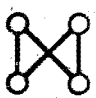
$$B_5 = -\frac{1}{30} \iiiii [2 \text{---} \text{---} \text{---} \text{---} \text{---} + 60 \text{---} \text{---} \text{---} \text{---} \text{---} + 10 \text{---} \text{---} \text{---} \text{---} \text{---} + 10 \text{---} \text{---} \text{---} \text{---} \text{---} + 60 \text{---} \text{---} \text{---} \text{---} \text{---} + 30 \text{---} \text{---} \text{---} \text{---} \text{---} + 30 \text{---} \text{---} \text{---} \text{---} \text{---} + 15 \text{---} \text{---} \text{---} \text{---} \text{---} + 10 \text{---} \text{---} \text{---} \text{---} \text{---} + \text{---} \text{---} \text{---} \text{---} \text{---}] d\vec{r}_2 d\vec{r}_3 d\vec{r}_4 d\vec{r}_5.$$



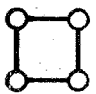
3



+



+



$$B_4 = -\frac{1}{8} \iiint [3 \{ \text{diagram 1} - 2 \text{diagram 2} + \text{diagram 3} \} + 6 \{ \text{diagram 4} - \text{diagram 5} \} + \text{diagram 6} + 3 \text{diagram 7}] d\vec{r}_2 d\vec{r}_3 d\vec{r}_4 = -\frac{1}{8} \iiint [-2 \text{diagram 8} + 3 \text{diagram 9}] d\vec{r}_2 d\vec{r}_3 d\vec{r}_4;$$

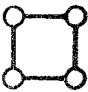
$$B_5 = -\frac{1}{30} \iiint [-6 \text{diagram 10} + 45 \text{diagram 11} - 60 \text{diagram 12} + 10 \text{diagram 13} + 12 \text{diagram 14}] d\vec{r}_2 d\vec{r}_3 d\vec{r}_4 d\vec{r}_5.$$

$$-\frac{\int \int f_{12} f_{13} f_{23} dx_2 dx_3}{\int \int f_{12} f_{13} f_{23} dx_2 dx_3} = \frac{-\int \int [ \text{triangle diagram} ] d\vec{r}_2 d\vec{r}_3}{\int \int [ \text{triangle diagram} ] d\vec{r}_2 d\vec{r}_3}$$

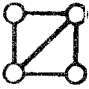
$$= \frac{\int \int f_{12} f_{13} dx_2 dx_3}{\int \int f_{12} f_{13} dx_2 dx_3}$$



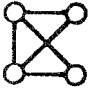
2



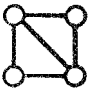
3



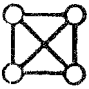
4



5



AND





AND



$$\begin{aligned}
\mathcal{R}_4(\mathcal{C}) = & \frac{1}{18} \sqrt{\sqrt{3}} \left[ 3 \left( \text{square} \right) + 2 \left( \text{square with diagonal} \right) + \left( \text{square with two diagonals} \right) \right] \\
& + \left( \text{square with diagonal} \right) + \left( \text{square with two diagonals} \right) \\
& + \left( \text{square with two diagonals} \right) \left[ d_1^2 d_2^2 d_3^2 d_4^2 \right]
\end{aligned}$$

$$B_4(f) = -\frac{1}{8} \iiint [3 \text{diagram}_1 + \{- \text{diagram}_2 + 2 \text{diagram}_3 - \text{diagram}_4 \} - 2 \text{diagram}_5] d\vec{r}_2 d\vec{r}_3 d\vec{r}_4.$$